THE BELL SYSTEM TECHNICAL JOURNAL
Vol. 59, No. 9, November 1980
Printed in U.S.A.

Loop Transients at the Customer Station

By R. L. CARROLL and P. S. MILLER

(Manuscript received April 16, 1980)

Electrical transients on the customer loop are of concern because they induce stress on customer terminal equipment, as well as on the station protector. To study this problem, we have recorded transient waveforms produced by lightning on a 10-mile loop in Washington, Connecticut, and have extracted information on peak current, peak voltage, polarity, rate of rise, decay time, and energy from the waveforms. The results are of significance to designers of protectors and station equipment.

I. INTRODUCTION

Design of modern station protectors and electronic station apparatus requires knowledge of the unwanted electrical transients that may appear on the telephone loop plant. Although previous studies[1-3] have provided empirical descriptions of voltage transients on various types of telephone plant, the data cannot be extrapolated to measurements at a customer station in a straightforward manner. The lack of data on current transients in loop-plant cable further restricts the usefulness of these studies for station and terminating equipment design purposes.

One approach for obtaining the desired environmental information is the development of an analytical model which, for instance, might represent the loop plant as a multiport network excited by random voltage or current sources. The complexity of the loop plant and the excitation sources, however, has restricted modeling efforts to a few simple cases.

To provide a more extensive set of data useful for establishing empirical descriptions of transients on the loop plant and for examining the validity of more complete analytical models now being developed, a program was initiated in which detailed measurements could be made at several Bell System station locations. Measurements at the first two sites have been completed and, although processing of data from the second experiment is not yet complete, a consistent picture

of lightning disturbances on loops has begun to emerge. This paper reports results obtained in the town of Washington, Connecticut.

II. SYSTEM, SITE, AND LOOP CHARACTERISTICS

2.1 Measurement equipment

Waveforms were recorded by automatic unattended oscilloscope/camera systems modified to produce nonlinear horizontal and vertical axes. (Subsequent to the Washington effort, digital measurement equipment was used to produce more precise measurements.) The systems were powered by a motor generator whose output was electrically isolated from the power service and equipped with standby battery capability. The oscilloscope vertical amplifiers provided 25-mHz bandwidth; the cathode ray tube phosphor and beam-brightening characteristics were optimized for transient observation.

An external trigger system sensitive to waveforms of both polarities caused a photograph to be taken when the input voltage exceeded 250 volts. The ring conductor of the monitored pair was connected to ground. Wideband nonlinear attenuators, driven by magnetic pick-ups, allowed measurement of current in this conductor from ±0.1 to ±3000 amperes. The tip conductor was connected to the trigger system and to a high-voltage probe for voltage measurement purposes. Voltages on this conductor were limited to ±2000 volts by a series string of gas tube surge arresters. There was a 0.4 second measurement window each time the equipment was triggered. A nonlinear time base was utilized to observe waveforms as short as a few microseconds (μs) or as long as several milliseconds (ms). As a result, only the first 2 ms of the sweep was of high resolution. Strokes subsequent to the first, if they were visible, were seen as impulses. Equipment recycle time was nominally one second. A diagram of the system, showing the major elements described here, is given in Fig. 1.

2.2 Study location and route characteristics

The Washington Exchange of the Southern New England Telephone Co. is located in the Berkshire Hills of western Connecticut, where a 355A step-by-step machine serves approximately 2000 main stations. Most of the stations are rural and located among hills up to 1450 ft altitude. National Weather Service statistics record 10 to 30 thunderstorm days per year in the area. The telephone plant is almost exclusively grounded metal sheath cable, the bulk of which is aerial. The local power system is delta, resulting in low 60-Hz induction and few high-current power contacts. Since water in the area is supplied by private well systems, station grounding electrodes cannot be connected to extensive metallic pipe networks such as are often present in suburban communities.

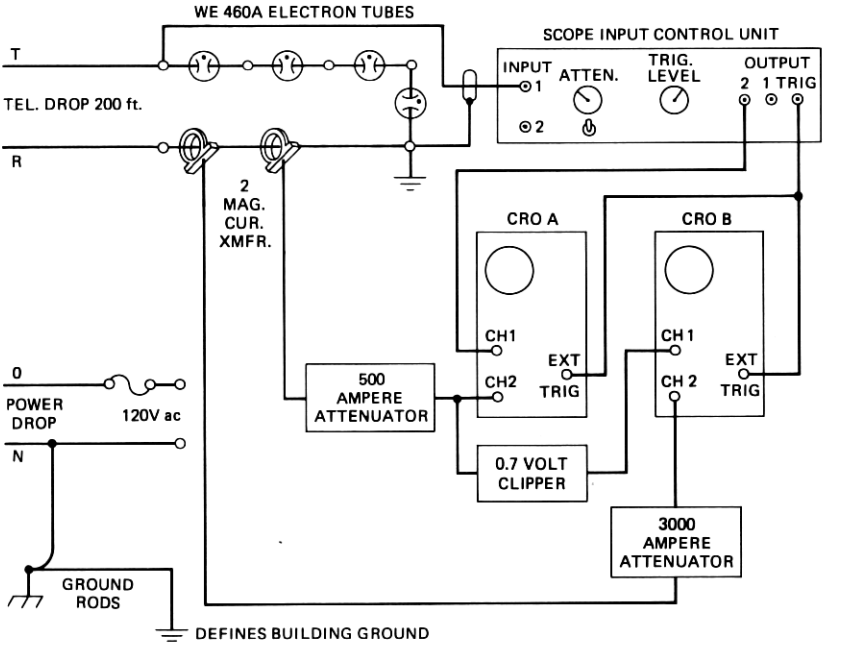

Fig. 1—Washington study instrumentation.

The cable to the monitoring location was aerial, in joint construction with a 4.8-kv delta power for approximately 95 percent of its length. One pair was monitored at the measurement location. This pair was H88 loaded and contained nine load coils. It left the central office in one of three cables on separate strands that proceeded for approximately 9 miles. At that point, two 50-pair cables were double-lashed for 1 mile. At a distance of 10 miles from the central office, the monitored pair entered a 25-pair PIC cable. This cable left the main route (on which route a single 50-pair cable extended an additional mile to the exchange boundary) and continued for a length of 0.3 mile. (The overall loop length, then, was 10.3 miles.) A 200-ft aerial drop* from a protected cable terminal equipped with 6-mil carbon blocks (prevalent in the area) provided service to the temporary structure that housed the measurement equipment. The same cable terminal also served three adjacent houses. One additional protected cable terminal serving three loops was located between the main route and the terminal serving the monitoring location.

The loop itself was 19-gauge, except for a short 24-gauge segment at the central office. It was one of the longest loops in the exchange; the

* The drop wire was type F, 4.3 ohms/conductor.

loop resistance, excluding terminations, was approximately 1500 ohms. For the purposes of the monitoring effort, the loop was terminated at the central office in two 550-ohm noninductive resistors center-tapped to ground, a resistive approximation to the normal line relay. Battery was not connected to the loop. The grounding arrangement at the measurement structure consisted of four driven ground rods, one at each corner of the structure (about 12 ft apart), connected by a common conductor and connected to the power ground rod installed by the power company. Measurements taken on several occasions indicated a ground resistivity of about 300 meter-ohms in the vicinity of the test location. Measurement of the isolated four-electrode driven telephone ground array indicated a resistance to remote earth of about 55 ohms. With the power ground rod and neutral reconnected (as they were during system operation), the ground resistance might be expected to drop considerably, since the pole transformer ground electrode, customer power grounds, and private water systems of the surrounding structures all paralleled the measurement structure ground.*

The two conductors of the monitored pair were connected to the measurement system as previously shown in Fig. 1. The conductor which terminated on the ground system was used to sense current via wideband current transformers; the open-circuited† conductor was used to sense voltage and to trigger the system for voltages > 250 V. The voltage measurements are a measure of the voltage across the nonconducting voltage limiter at a subscriber station in the presence of current flow through the other (zero impedance or shorted) voltage limiter. The current measurements may be interpreted as the short-circuit current to ground for those events in which the voltage on the other conductor exceeded 250 V.

2.3 Period of operation

The system was installed on May 22, 1975, and deactivated on September 15, 1975. During this period, 23 thunderstorm days occurred, according to observers at the Washington central office. There were 1230 recorded surges of satisfactory optical quality. This yielded an average of 53 surges per thunderstorm day; more than one hundred surges were recorded on several of the days. Since the system ran out of film during one storm and was out of service during one other storm, the actual number of surges which occurred during the monitoring interval was higher by an amount which cannot be determined.

---

* Three customers were served from the transformer supplying power to the measurement location.

† Input of the trigger system was approximately 20 kilohms to the single-point system ground.

III. DATA RECORDING

3.1 Data digitization

The 35-mm film records of each event were enlarged and digitized. The error of digitization was judged to be no worse than one division out of the 30 available on the vertical (voltage or current) axis or of the 50 divisions available on the horizontal (time) axis. If a maximum error in the electronics of ±3 percent is assumed, this implies accuracy on the order of 10 percent in amplitude data.

3.2 Data categories

Information on the following items was extracted from the digitized records or calculated from the data:

(*i*) Waveshape.
(*ii*) Peak measurements:
  (a) Peak voltage.
  (b) Peak current.
  (c) Polarity of peak measurements.
  (d) Correlation of peak voltage and peak current.
(*iii*) Voltage rate of rise.
(*iv*) Decay time and energy.
(*v*) Time between surges (interarrival times).

In the sections which follow, the definition and significance of each category are discussed and the results summarized. More detailed statistical analyses of the data on peak voltage, peak current, decay time, and energy are provided in the appendix.

IV. DESCRIPTION OF DATA AND STATISTICAL SUMMARIES

4.1 Waveshape

Typical waveforms, showing voltage and current as functions of time, are illustrated in Fig. 2a to 2k. The first 800 microseconds of digitization from photographic records are shown in each plot.*

In previous monitoring efforts, recorded voltage waveshapes have been observed to be approximately damped sinusoidal [$Ae^{-\alpha t} \sin(\beta t + \phi)$] or double exponential ($Ae^{-\alpha t} - Be^{-\beta t}$), for $t > 0$. Of the waveforms recorded in Washington, however, none appeared to be well approximated by a double exponential.

Many of the lower current events are typified by figs. 2a to 2g, which at first glance appear to be damped sinusoids. Closer examination, however, reveals that they are somewhat more complex, as the spectrum of Fig. 3 (computed via discrete Fourier transform techniques) indicates.† In this particular case, the time function may be approxi-

* The entire records were available for analysis purposes.
† Note the upper and lower half-power points are approximately 8.5 and 2.8 kHz, respectively.

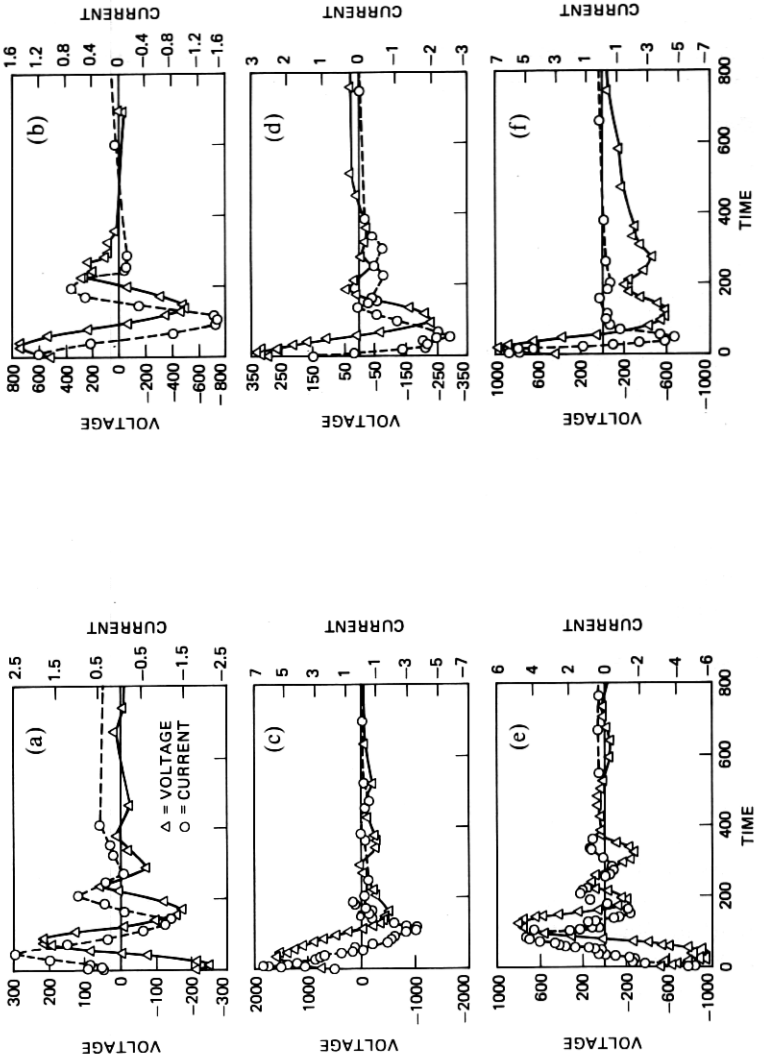
(a)
(b)
(c)
(d)
(e)
(f)
Δ = VOLTAGE
○ = CURRENT
VOLTAGE
CURRENT
TIME

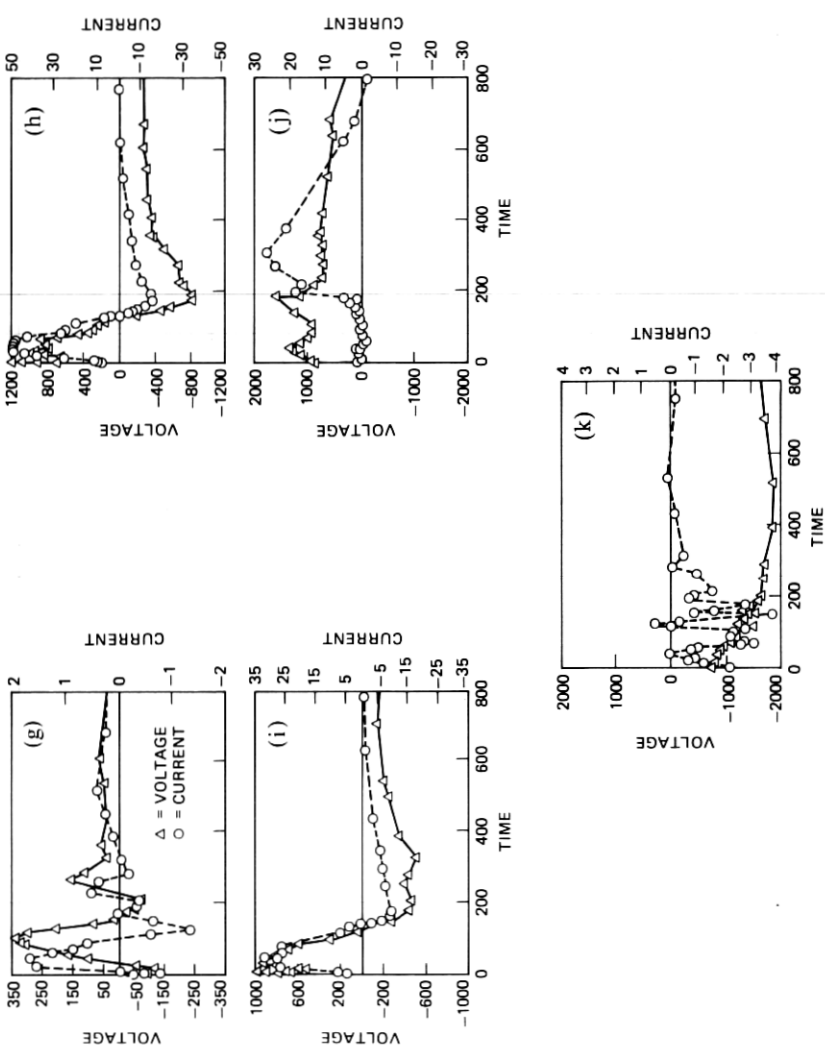

Fig. 2—Representative waveforms.

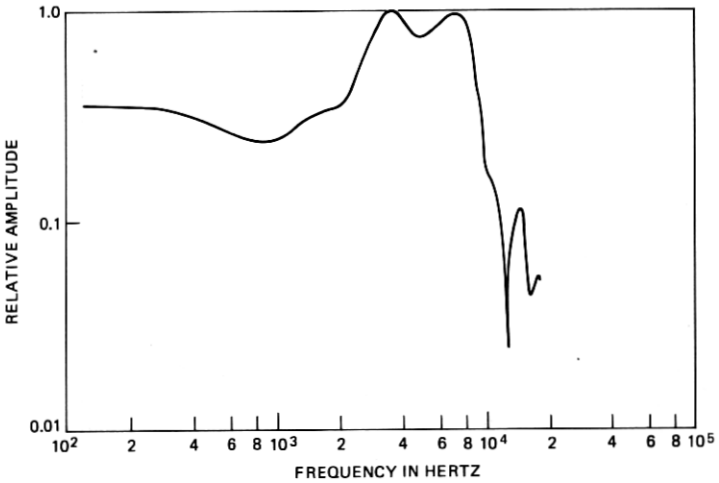

Fig. 3—Computed spectral magnitude of voltage trace of Fig. 2e.

mated by a function having two damped sinusoidal components, with frequencies of 3.5 and 7.0 kHz and a decay time constant of about 250 μs. A function based on these parameters is shown in Fig. 4 and is a reasonable approximation to Fig. 2e. Detailed spectral analysis of each event was not practical because of the analog measurement system used.

A second type of waveform is illustrated in Figs. 2h and 2i. No phase shift (between voltage and current) is evident during early portions of these events. In this study, such behavior was always associated with relatively high currents, presumably from strokes physically close to the monitoring location. It was much less common than the "oscillatory" response.

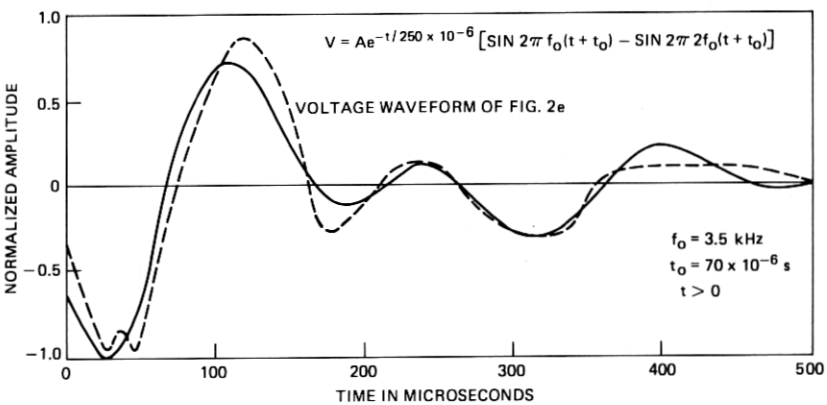

Fig. 4—Approximation to Fig. 2e on the basis of two damped sinusoids.

Other waveforms such as those shown in Figs. 2j and 2k could best be described as "complex." They cannot be described by a simple analytical expression. No waveforms attributable to 60-Hz disturbances induced by the power system were detected, although coupling of lightning strokes from the power system to the telephone conductors almost certainly occurred.

4.2 Peak measurements

4.2.1 Peak voltage

The peak voltage of a surge was defined as the maximum voltage magnitude (either positive or negative) observed during the surge. As previously indicated, this voltage on the unterminated conductor was measured in the presence of current flow to ground in the other conductor. The relatively low currents, low rates of rise (discussed later), and low ground resistance indicate that, in most cases, the extent to which these voltages differed from those that would have been obtained in the absence of current flow is small. The peak voltage measurement is of interest in that it determines whether or not a voltage limiter having a particular sparkover voltage will operate during a given electrical surge. It also provides a description of the magnitudes of surges not limited by a protective device, which may be imposed on station apparatus. The absolute peak voltage data are shown on a logarithmic scale in Fig. 5, plotted vs a normal probability scale. Summary statistics are also given. Here and in many of the plots which follow, the normal probability scale is used to highlight the tails of the distribution. The upper tail, in many cases, is most relevant to protector operation.

A median of 381 V and maximum of 1894 V were observed. Several theoretical distributions were considered as models for the peak voltage data; this analysis is described in the appendix. The distribution that "best" modeled the peak voltage data was a truncated lognormal distribution which had a theoretical minimum of 25 volts and which assumed that 38 percent of the observations were below 250 volts and, therefore, could not be observed. Although this was the best of the models considered, the fit in the upper tail was judged to be inadequate to allow the theoretical distribution to be very useful in terminating equipment design.

4.2.2 Peak current

The peak current of a surge was defined as the maximum absolute current magnitude observed during the surge. When a gap-type voltage limiter conducts current, the peak current flow is of interest, since the life of the limiter can normally be partially specified in terms of this parameter. The current information is also useful in determining the

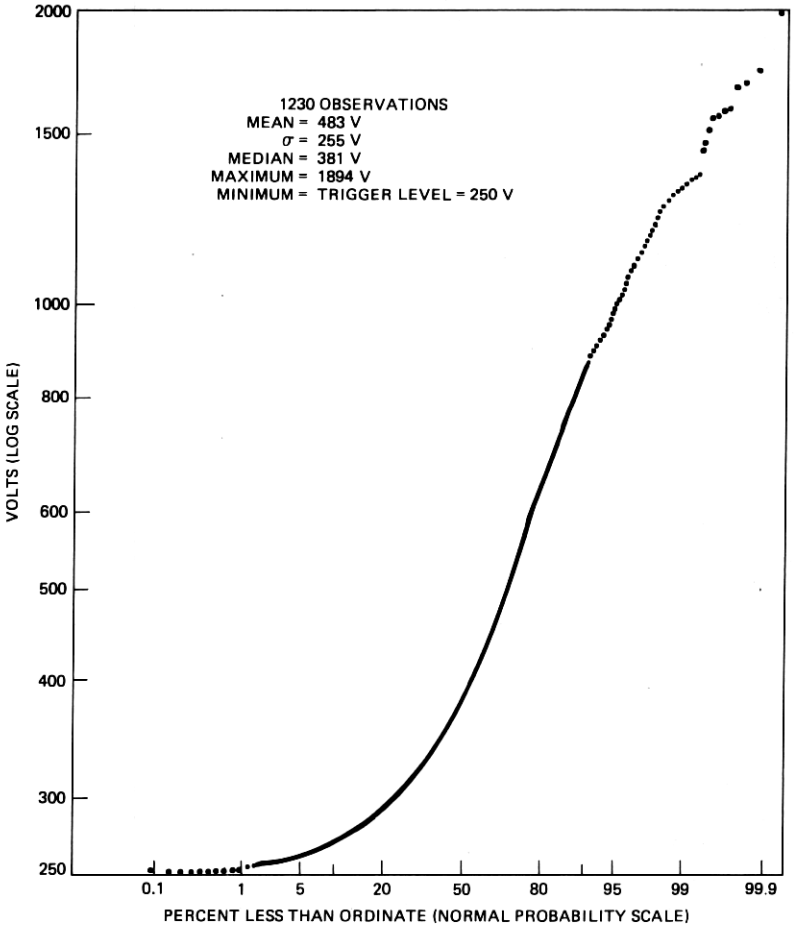

Fig. 5—Absolute peak voltages measured at Washington.

peak short-circuit capability to be used in testing station apparatus. As indicated in Fig. 1, current measurements were made during the Washington program by shorting one loop conductor to ground and sensing currents through two transformer pickups. The low impedance transformers were applied to nonlinear wide bandwidth attenuators, which coupled the signals to oscilloscope systems covering the range of 0.1 to 3000 A. One transformer covered the 1 to 3000-A range and was intended to provide accurate measurements of lightning surge current waveforms. The other transformer covered the 0.1- to 1-A range and was intended to provide an indication of low-level currents induced by the power system.

As in the case of the voltage data, the current waveforms were complex and aperiodic. No events attributable to steady-state induc-

tion from power lines were detected. The peak current associated with each photographic record was determined. The peak current data (on a scale which is logarithm of one plus the current measurements) are plotted vs a normal probability scale in Fig. 6. This figure also contains summary statistics. The median of the 1230 observed peak currents was 1.2 A, and the maximum observation was 59 A. To model these data, only surges having peak current greater than one ampere were considered, because it was judged that data below this point may not have been of satisfactory precision. The best model for the subset of 742 peak currents greater than 1 A was a truncated lognormal distribution.

The right-hand scale of Fig. 6, which shows predicted events at the Washington field site over a 20-year period, was obtained by multiply-

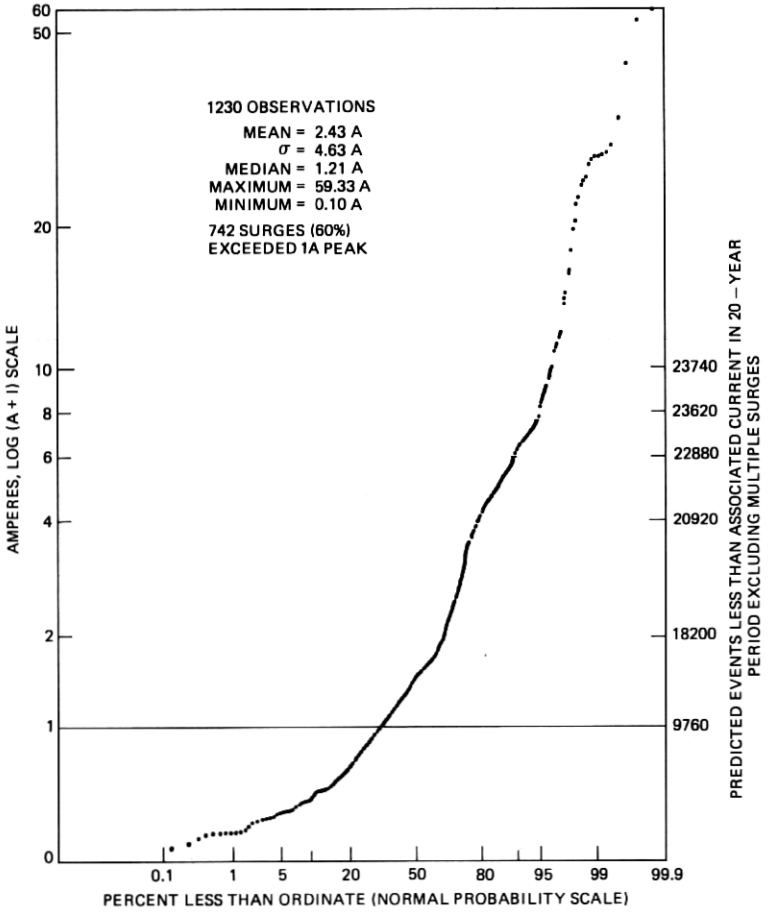

Fig. 6—Absolute peak currents measured at Washington.

ing by 20 the number of observed events that were less than the number of amperes shown on the left-hand scale. For example, 488 observed events were less than one ampere and, multiplied by 20, this would equate to 9760 in a 20-year period. The implicit assumption is that the total number of events (1230) is the number that would occur in one lightning season. Though a simplistic approach, this provides an idea of the large number of events which a protector device must survive during a nominal 20-year life. More detail on the statistical analysis of peak current data is given in the appendix.

4.2.3 Polarity of peak measurements

An examination of the polarity of peak voltages (telephone conductor to ground) indicated that 68 percent of the measurements were negative. When the subset of 742 events having peak currents exceeding one ampere was considered, 51 percent were found to have negative peak current measurement. In this instance, no advantage could be taken of any polarity sensitivity of the life characteristic of a voltage limiter device.

4.2.4 Correlation of peak voltage and current

The empirical relation between peak voltage, v, and peak current, i, was considered for the 742 events with peak currents exceeding 1 A. In previous studies, such as in Refs. 1 and 2, measurements of voltage were taken, but not of current. Under environmental conditions that are identical from one surge to the next, voltage and current would be related to each other by a constant multiplier. It was expected that the environment would not remain constant throughout the study, since conditions would vary as the storm moved. However, it was hoped that the correlation between voltage and current would be high enough to allow inference from voltage measurements taken in previous studies to measurements of current.

The sample correlation coefficient between v and i was found to be 0.36, which (for a sample as large as this) is highly significant statistically. The correlation is too high to hypothesize independence, but too low to be of value in determining a linear relationship between the two quantities.

The v–i scatter plot, shown on a logarithmic scale in Fig. 7, shows the lack of a definitive relationship. Since the ranges of peak voltages and currents were so large, logarithmic transformations seemed worth investigating. The correlation between log peak voltage and log peak current was 0.37. This value is very close to the correlation between peak voltage and current before transformation. This implies that large voltages and currents varied from a linear relationship by about the same amounts as did smaller values and thus did not tend either to inflate or deflate the sample correlation coefficient.

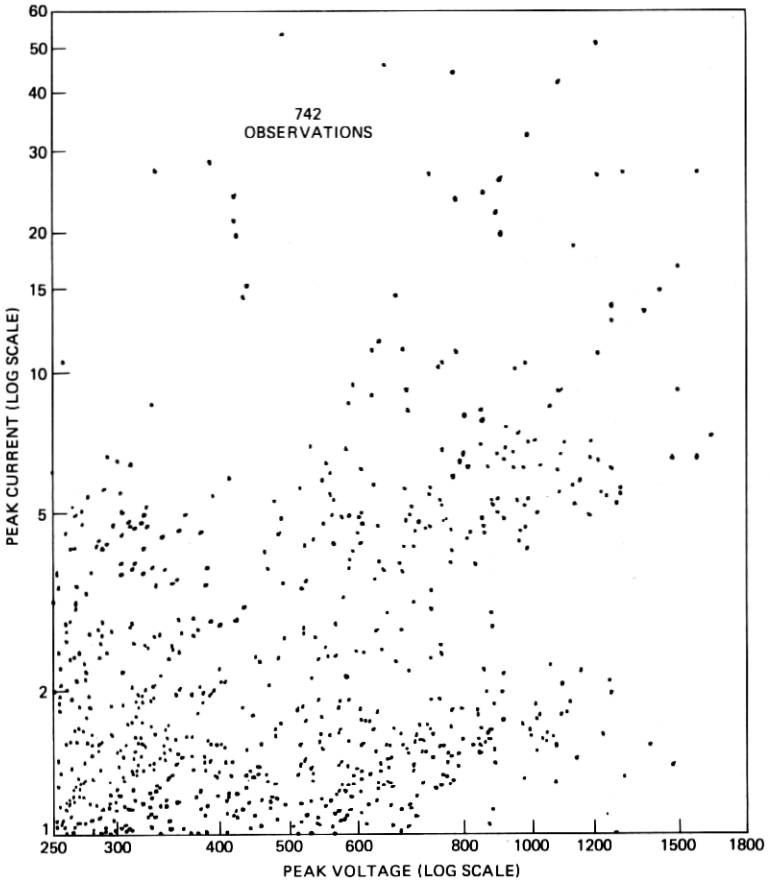

Fig. 7—Scatter plot of peak current vs peak voltage.

An examination of only those points in Fig. 7 corresponding to surges having peak currents in excess of 5 A suggested that the correlation between peak voltage and current might be much lower than 0.36. This was found to be the case. For this subset of 120 surges, the sample correlation between peak voltage and current was only 0.04.

Next, the hypothesis was examined that data within a storm might be more homogeneous than the pooled data from the entire storm season. If a few particular patterns of storms could be identified, this might be useful in making inferences. Two storms* were examined individually. The first storm, consisting of 116 surges, had a median peak voltage of 814 V as compared to the overall median of 381 V. The second storm of 80 surges had a median peak voltage of 304 V. Each

* For this analysis, a storm was arbitrarily defined as having ended when a period of 120 minutes or more occurred containing no photographic records.

of these storms was certainly different from the other and from the sample as a whole. However, neither storm provided a better fit of the peak voltage or currents to any of several theoretical distributions considered; the correlation between peak current and peak voltage remained about 0.4 for each.

4.3 Voltage rate of rise

The voltage rate of rise of a transient waveform, expressed in V/μs, has a strong effect on the breakdown voltage of many gap-type voltage limiters and on the withstand capability of certain station apparatus. Because of the complex waveshapes of the Washington recordings, rate of rise has been defined in this paper as the derivative of the magnitude of the voltage waveform at the first crossing of a specified threshold. This was computed empirically as the slope between the two points on either side of this crossing. Levels of 300 and 500 V were selected as thresholds that are relevant to protector operation. Since many surges never exceeded these levels (i.e., 300 or 500 V), the numbers of events available for analysis were reduced to 419 and 149, respectively.

Rate of rise data for the 300- and 500-V thresholds (logarithmic scale) are plotted vs a normal probability scale in Fig. 8, and summary statistics are given. As might be expected, the rate of rise distribution is higher at 500 V for that subset of surges which reached the 500-V threshold. However, the maximum of 129.1 $v/\mu s$ was observed for the distribution at 300 V. The percentage of observations taken at the 500-V threshold which were less than 100 $v/\mu s$* was 98.6 percent.

4.4 Equivalent decay time and energy

The decay time of a lightning surge is an important indicator of the stress imposed on equipment and thus of equipment life. The decay time of a double exponential waveform is defined as the time interval from zero to the point at which the wave has decayed to one half its maximum value. For the waveforms observed in the Washington study, this definition is inadequate, because the half-value point is achieved on multiple occasions. To relate the present data to that obtained in Refs. 1 and 2, a new definition has been constructed as indicated below.

Consider a double exponential wave in which the rise time is very much shorter than the decay time. For the purpose of the decay time calculation, the wave may be approximated accurately by

$$v(t) = v_p e^{-t/\tau_D}, \qquad t > 0,$$

* Common practice in the protector community is to evaluate voltage limiters at 100 $v/\mu s$.

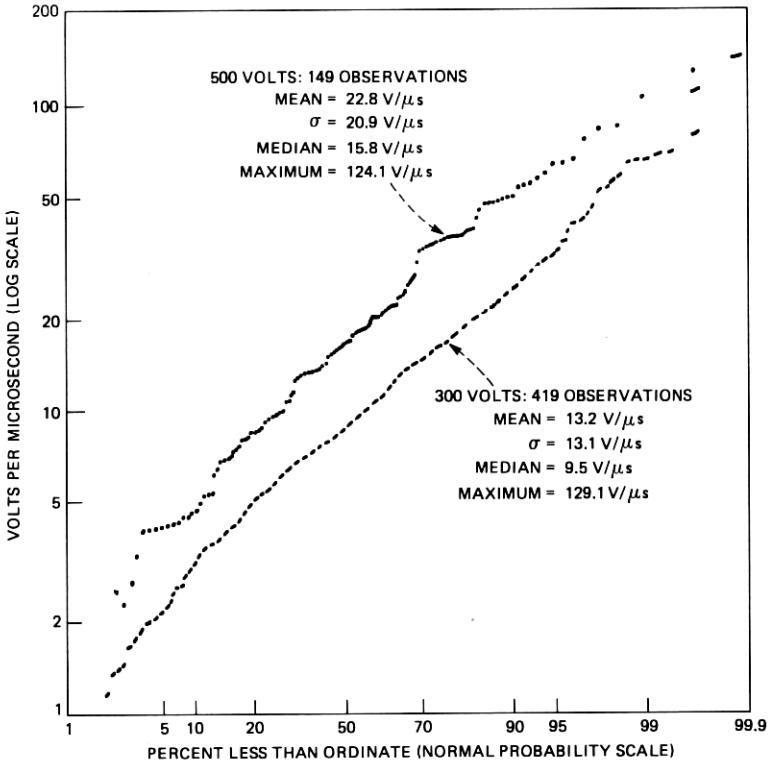

Fig. 8—Voltage rate of rise at first crossing of 300 and 500 V.

where $v(t)$ is the voltage at time t, v_p is the absolute peak voltage, and τ_D is the decay time constant. Integrating both sides of the equation with respect to t over the range $(0, \infty)$ and solving for τ_D, one can show that

$$\tau_D = \frac{1}{v_p} \int_0^\infty v(t)dt.$$

A generalized equivalent decay time constant can then be defined for an arbitrary waveform and peak voltage by

$$\tau_{\text{equiv1}} = \frac{1}{v_p} \int_0^\infty |\, v(t) \,| \, dt.$$

(The absolute value enters because $v(t)$ is no longer always positive.) For the exponential case, τ_{equiv1} equals τ_D. A similar calculation based

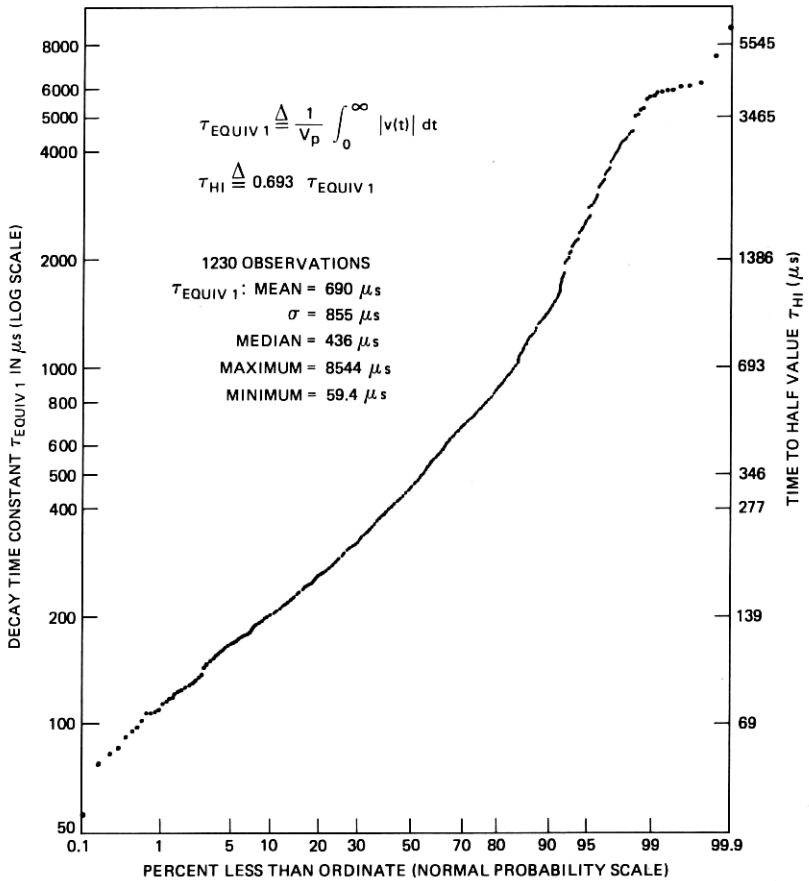

Fig. 9—Equivalent decay-time constant based on $\int |v|\,dt$.

on the square of the voltage waveform* yields

$$t_{\text{equiv2}} = \frac{2}{v_p^2} \int_0^\infty v^2(t)dt.$$

Equivalent decay time constants based on current are obtained by substituting the current waveform and peak, $i(t)$ and i_p, for $v(t)$ and v_p, respectively, in the above equations.

These equivalent decay constants are defined such that a given waveform is associated with an equivalent decay time which is identical to that calculated for an exponential wave having the same peak value as the given waveform. This allows comparison of the present wave-

* Energy dissipated in a resistive load is proportional to $\int v^2 dt$ or $\int i^2 dt$.

forms, which are complex in waveshape, with previous data, as in Refs. 1 or 2, which have been primarily exponential. Figures 9 and 10 are plots of the decay time constants, based on voltage and squared voltage (logarithmic scales), respectively, versus a normal probability scale. The two distributions are similar; the median of the distribution based on v is somewhat higher than that of the distribution based on v^2, but the maximum of the v^2 distribution is the higher one.

Both equivalent decay time constants may be further related to previous data by defining the equivalent time to half value, τ_H, as $\tau_H = 0.693\ \tau_{equiv1}$ (or τ_{equiv2}), which is derived from the relation between these two quantities in the exponential case. The right-hand vertical axes of Figs. 9 and 10 are scaled in this manner.

Energy is defined directly as $\int_0^\infty |x(t)|\,dt$ or $\int_0^\infty x^2(t)\,dt$, where $x(t)$ may represent either the voltage or current waveform. Summary

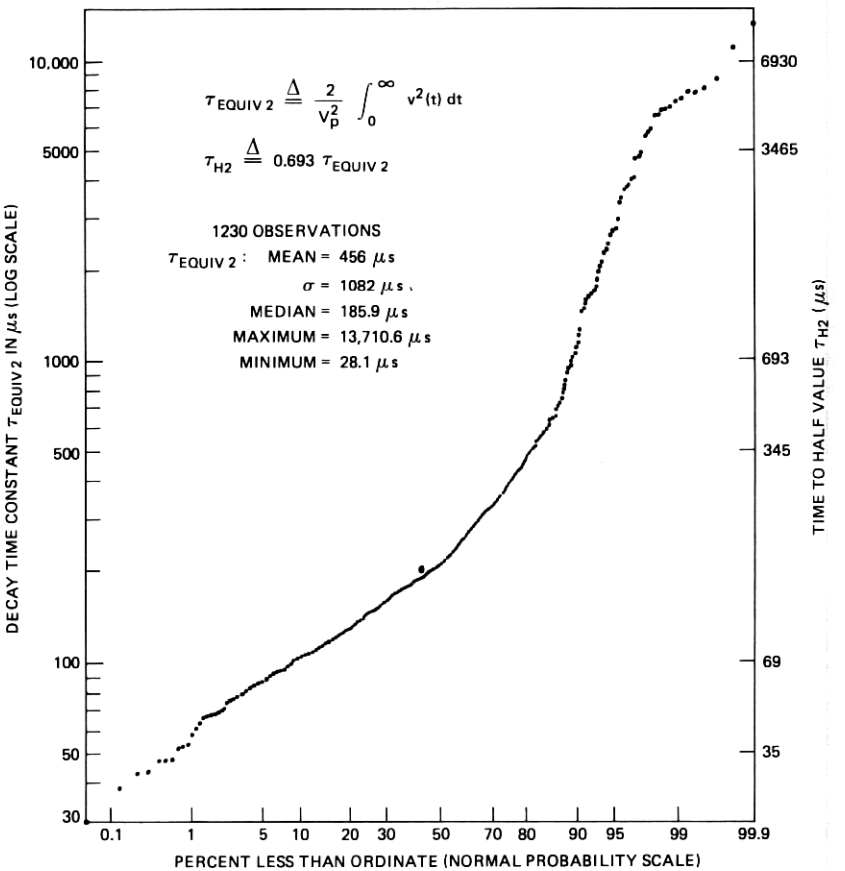

Fig. 10—Equivalent decay-time constant based on $\int v^2\,dt$.

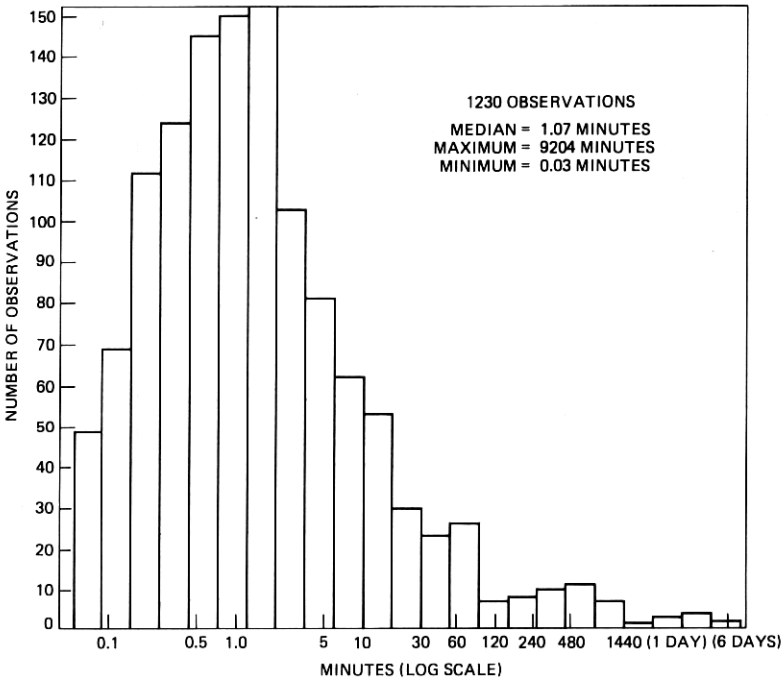

Fig. 11—Times between surges. Histogram of logs of time shows in units of minutes.

statistics and descriptions of these and other related data are contained in the appendix. The decay time distributions are similar to each other, whether based on v, v^2, i, or i^2. All are highly positively skewed. The means of the distributions based on i and i^2 are somewhat higher than those based on v or v^2; this is possibly due to measurement inaccuracies in the tails of the current waveforms, caused by decreased resolution at low current levels.

4.5 Times between surges (interarrival times)

The distribution of times between the arrival of successive surges, or interarrival times, is of interest in the design of surge monitoring equipment and in the characterization of the thunderstorm process. Figure 11 is a histogram of the logarithms of times between surges recorded at the Washington site. The most straightforward assumption, a Poisson arrival process, leads to an exponential distribution of times between surges. The measured times do not support this assumption. Rather, a lognormal appears to be a better fit to the data. However, the histogram in Fig. 11 has a right-hand tail which is much too long to belong to the normal distribution. (The distribution of logarithms of times would be normal if times were distributed as a

lognormal.) It is reasonable to hypothesize that there may be two different processes involved: one a random process that determines the arrival of storms and a second that is dependent on the state of the first and that determines the arrival of surges within a storm. In these data, the only way to differentiate between interstorm times and intrastorm surge arrival times is by the length of time. Times between storms should generally be longer than times between surges within a storm.

Before the data of Fig. 11 had been examined, it was thought that two hours was a reasonable cutoff point between intrastorm and interstorm times. Figure 12 is a plot of all times less than two hours on a logarithmic scale vs a normal probability scale. The curve is close to a straight line, except for the upper tail. This plot can be interpreted as a lognormal probability plot where a straight line would indicate a

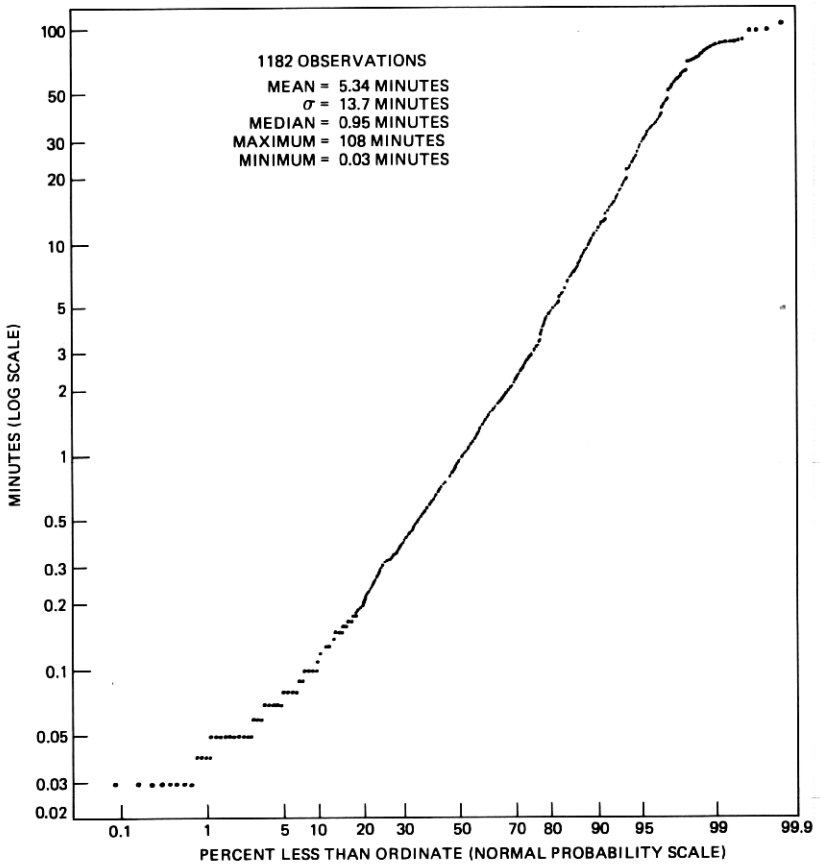

Fig. 12—Times between surges for times less than 2 hours.

good fit of the data to the lognormal distribution. (Times were measured in hundredths of a minute, which accounts for the discrete appearance of the lower tail.)

The curvature of the upper tail could possibly be eliminated if some of the points beyond the two-hour cutoff were actually intrastorm times and were included in the plot. Since it is impossible to tell which of the 48 points greater than two hours are intrastorm times, it was decided to ignore them and to treat the times less than two hours as observations from a right-truncated distribution. Varying numbers of observations were considered truncated, from 0 to the largest possible number, 48. Figure 13 is a lognormal probability plot showing the data as if there were 20 observations (i.e., 2 percent) greater than two hours which are not shown. The upper tail is much straighter here than in

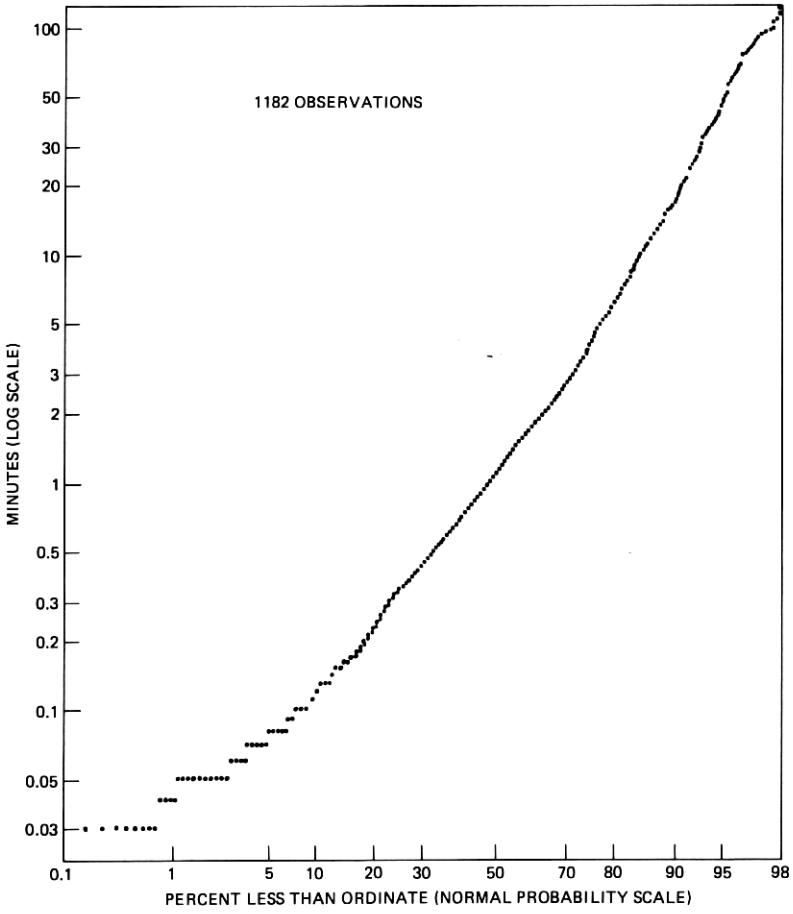

Fig. 13—Times between surges assuming 2 percent truncation.

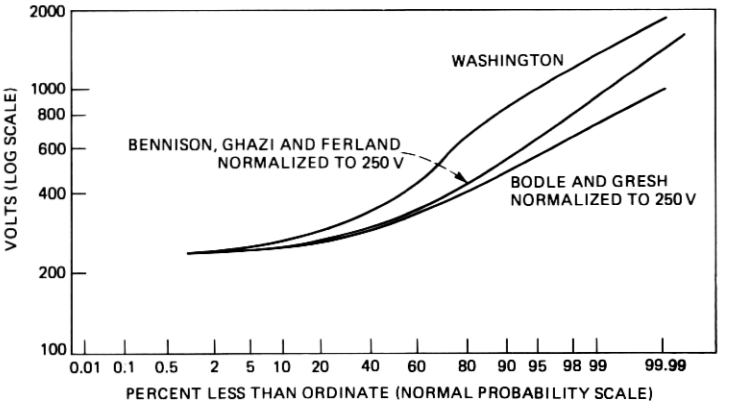

Fig. 14—Comparison of peak voltage data.

Fig. 12. In this scenario, the maximum observed time between surges within a storm would be expected to be about 20 hours. Therefore, intrastorm and interstorm time distributions would overlap at least in the range of 4 to 20 hours.

V. COMPARISONS WITH PREVIOUS DATA

It is useful to compare the Washington loop plant data with those of previous studies conducted on outside plant toll facilities and/or trunk facilities, as documented by Bodle and Gresh (BG) in Ref. 1 and by Bennison, Ghazi and Ferland (BGF) in Ref. 2. Plots of the most severe peak voltage distributions reported by these authors and renormalized to a 250-V threshold are given on a logarithmic scale versus a normal probability scale in Fig. 14 along with the Washington peak voltage data. The Washington data indicate a more severe voltage distribution than was observed during studies at locations other than customer stations. The peak voltage distribution is a measure of the severity of the electrical environment and is useful for estimating the number of times a protector will operate during a thunderstorm.

Also of interest is the average number of events per thunderstorm day exceeding given voltages. These distributions may be obtained from the BG and BGF data by calculating the average number of surges exceeding 250 volts per thunderstorm day and scaling the observed distribution of peak voltages by this number. The curves of Fig. 15 show these results. From this figure, it may be seen that the higher Washington voltage distribution and the increased number of surges per day exceeding 250 V combine to produce a considerably more severe protector environment than observed in the BG and BGF data.

Decay times to half value from the Washington, BGF, and BG studies are shown in Fig. 16 on a logarithmic scale vs a normal probability

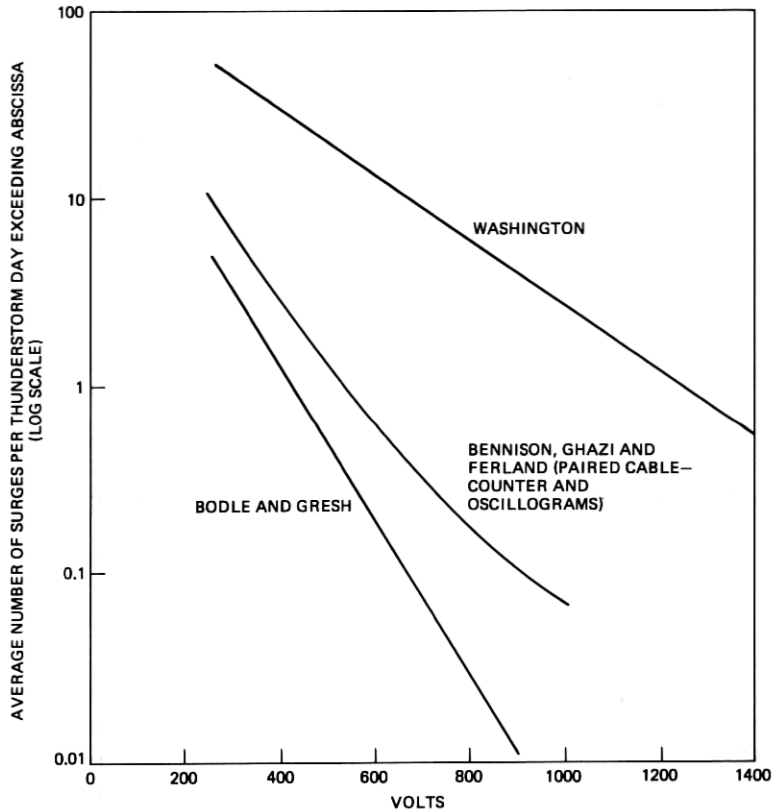

Fig. 15—Comparison of surges per thunderstorm day exceeding voltage thresholds.

scale. The Washington data are less severe than those found by Bodle and Gresh, up to the 90-percent (or 1000-μs) point. The Washington data range beyond the BG distribution at that point and also beyond the more severe BGF data at approximately the 98-percent, or 3500-μs, point. The Washington data indicate the possible presence of a few surges with extended decay times, when waveshapes of the type observed in the Washington loop plant are encountered.

Comparative rate of rise data are presented in Fig. 17 on a logarithmic scale vs a normal probability scale. It is clear that the rate of rise distribution in Washington is considerably more severe than that reported by BGF.

VI. SUMMARY

Current and voltage transients at the customer end of a telephone loop in Washington, Connecticut, were recorded for events exceeding 250 V. The quantities peak voltage, peak current, voltage rate of rise,

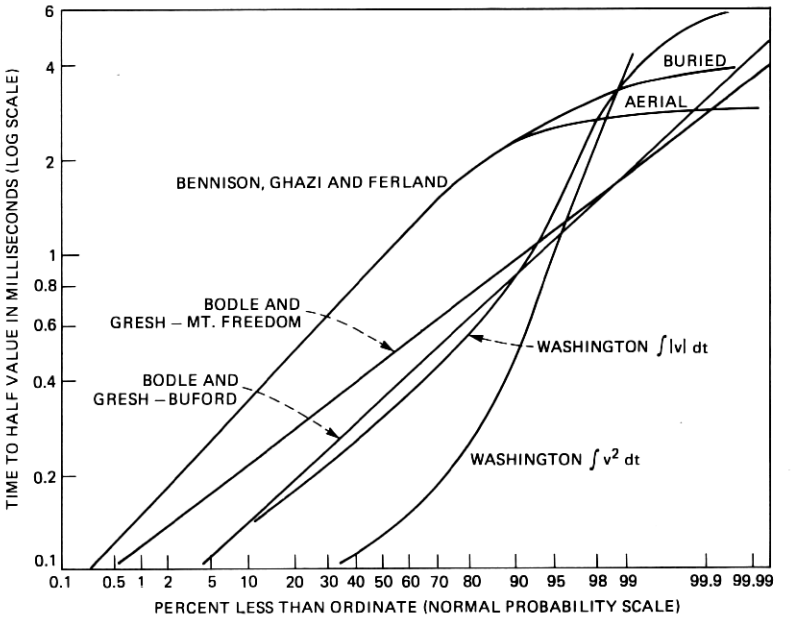

Fig. 16—Comparison of decay-time data.

decay time, energy, and time between events were derived for each recorded surge and were statistically analyzed. The voltage and current waveshapes did not correspond to the double exponential waveshape familiar from trunk studies, nor could they, in general, be classified as simple damped sinusoids.

The peak voltage distribution was found to conform best to a truncated lognormal distribution. Although this was the best model of several distributions considered, the fit was judged inadequate to be very useful in the design of terminating equipment. The median of the distribution was 381 V and the observed maximum was 1894 V. The peak current data were well modeled by a truncated lognormal distribution. Sample statistics of the observed currents were a median of 1.2 A and a maximum of 59 A. In both the peak voltage and peak current data, neither polarity showed a significant predominance over the other. The correlation between peak voltage and peak current was not strong enough to be useful.

Voltage rate of rise was measured at thresholds of 300 and 500 V. The maximum observation was 129 $v/\mu s$ (at 300 V). Equivalent decay times were found that ranged beyond corresponding data for trunks, the upper ends of the Washington distributions being more severe than the corresponding data for trunks observed in the Bodle and Gresh[1] or Bennison, Ghazi and Ferland[2] studies. The 90-percent point

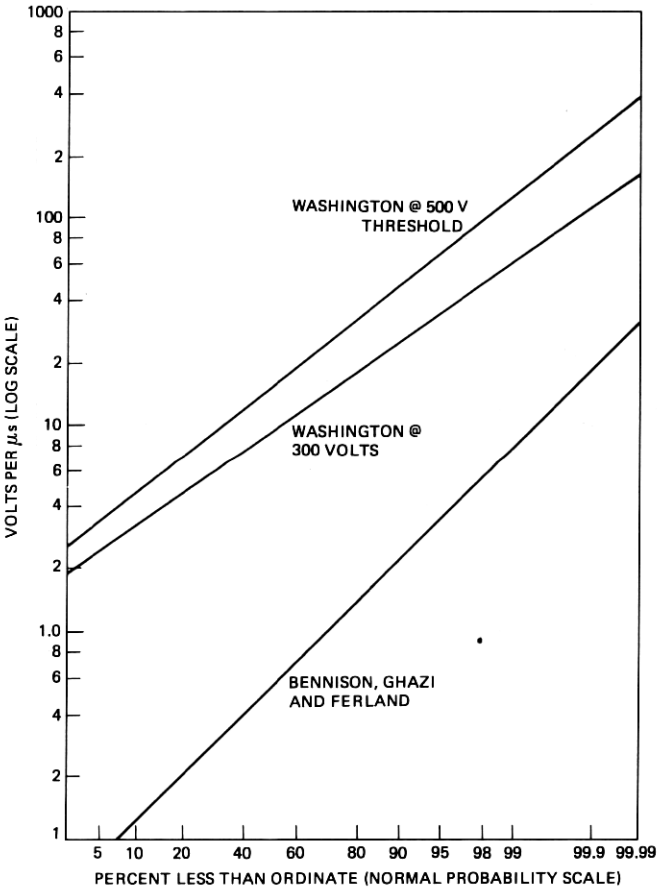

Fig. 17—Comparison of rate of rise data.

at 1000-μs observed by Bodle and Gresh was found to be in reasonable agreement with the Washington decay time data.

VII. ACKNOWLEDGMENTS

A program of this magnitude necessarily involves a number of key personnel. Credit for revitalization and modification of the system equipment (such as the signal compressors and sweep modifications) belongs to R. F. Youhas and W. F. Lichtenberger. Mr. Lichtenberger was responsible for organization of the data digitization program, while E. T. Lipinski developed numerous software programs for interpretation, organization, and storage of the digitized data. Bernie Petronis and Ernie Veihlman of Southern New England Telephone provided indispensable help in site preparation, route documentation, and equipment maintenance. Special thanks are due to G. W. Benz of Southern

New England Telephone, who provided the operating company support that made the program possible.

APPENDIX

Statistical Analyses of Peak Voltage, Peak Current, Decay Time, and Energy Data

Summary statistics and key points of the statistical analyses of several variables derived from the Washington data were given previously in the body of this paper. This appendix contains more detailed discussions of three of these variables, peak voltage, peak current, and decay time constants. Expected peak voltages are a critical factor in the design of terminal equipment. Moreover, in the design of protective devices, it is important to be able to estimate how many times the device will operate and to what current it will be subjected. Peak voltage is a determinant of how many times a protective device operates and, given that it does operate, peak current is a primary factor in determining its lifetime. If these two quantities could be modeled theoretically, this would be useful in determining specifications for the design of protectors and terminal equipment. The modeling of peak voltage and peak current by theoretical distributions is described in Sections A.1 and A.2. The methodology is summarized for possible future use as a guide in further studies of this type.

Section A.3 contains descriptions and comparisons of equivalent decay time constant and energy distributions obtained from the voltage and current waveforms. The decay time of a surge is an important indicator of the stress imposed on equipment and thus of equipment life. Information is provided on four separate decay time distributions, based on v, v^2, i, and i^2, and on the four corresponding energy distributions. Attempts to model these data with theoretical models were unsuccessful and are not reported here.

A.1 Peak voltage

Peak voltages were defined for each surge as the absolute maximum value of the observed voltage waveform. Since measurement of a surge began when the voltage reached a 250-V threshold, no peaks less than 250 V were recorded. Thus the distribution of observed peak voltages must be considered truncated, since surges having peaks less than 250 V would not have been measured.

A histogram of (absolute) peak voltages is shown in Fig. 18. The figure is scaled to include 98 percent of the 1230 observations; therefore, the maximum of 1894 V* is not shown. These data were also shown

* Observation of the photographic record confirmed that the event having peak voltage of 1894 did not operate the string of 460A gas tubes used to limit voltages on the "open circuit" conductor to ≈2000 V or less.

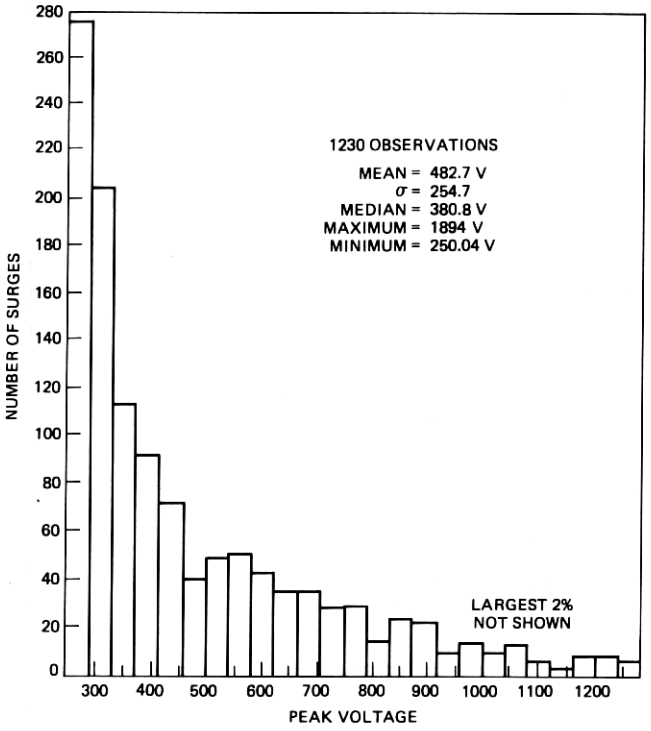

Fig. 18—Histogram of peak voltage.

earlier in Fig. 5, which can be interpreted as a lognormal probability plot. The minimum peak was 250.04 V. The median peak voltage was 380.8 V, and the mean and standard deviation were 482.7 and 254.7 V, respectively. (The corresponding statistics for the set of 742 surges with peak current greater than 1 A were a median of 475 V, mean of 555 V, and standard deviation of 285 V.)

Several distributions were considered as possible theoretical models for peak voltage (and for peak current, described in the following section). These included the exponential, Weibull, gamma, extreme value, truncated extreme value, lognormal, and truncated lognormal distributions. Estimates of parameters for each of these distributions were made from the data. The method of estimation in most cases was to regress the ordered data on theoretical quantiles (as in a probability plot). Many two-parameter distributions have the property that they can be reexpressed in a "standardized" form by the subtraction of a location parameter (μ) from each observation, or from a specific function of the observation, and division by a scale parameter (σ). Therefore, μ and σ can be estimated in such cases as the y-intercept and slope, respectively, of the best straight line fit between the ordered

observed values (y-axis) and the standardized theoretical values (x-axis). In the case of the gamma distribution, the method of moments was used to estimate the parameters.

The distributions were compared to one another on the basis of the value of the Kolmogorov-Smirnov (K-S) statistic, which is the maximum absolute deviation between the empirical and fitted cumulative distribution functions. Correct application of the K-S statistic requires that parameters of the hypothesized distribution are available independently of the data. Estimation of the parameters from the data, as was done here, increases the probability that the K-S test will not detect a difference between empirical and theoretical distributions. However, when the sample size is the same for each test, the K-S test statistic should give a fairly objective comparison among the different distributions.

Among the models in which the theoretical lower limit was assumed to be 250 V, the Weibull and gamma distributions provided the best

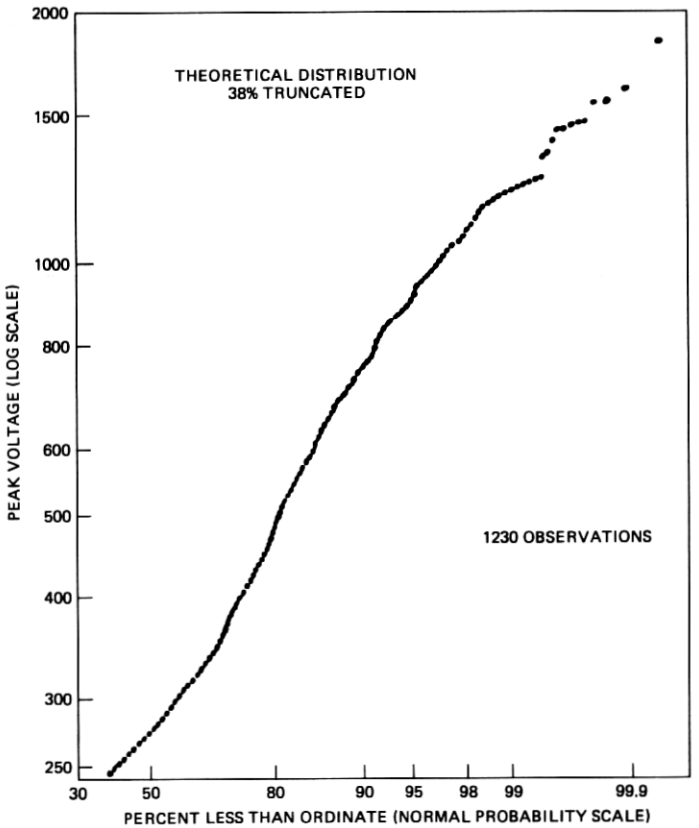

Fig. 19—Peak voltage assuming 38 percent truncation.

fits. However, the K-S test rejects both of these distributions as adequate fits to the data at the 1 percent significance level.

The truncated lognormal distribution proved to be the best model of any considered. This model assumed that some portion of the data (below 250 V) had been left-truncated. Truncated lognormal distributions having theoretical lower limits in the range of 0 to 250 V in steps of 25 were considered. For each, the degree of truncation which allowed the optimum fit to the peak voltage data was found by comparing integral percentages between 0 and 99 percent truncated. The K-S test statistic could not be used to compare distributions having different degrees of truncation. Since estimates of parameters were made from the data, the K-S statistic approached 0 as the degree of truncation increased. The criterion which was used to determine the degree of truncation, therefore, was the mean square error of the regression of the data on the theoretical quantiles. The K-S statistic was then computed for the model having the optimum degree of truncation.

The best model found, based on the K-S criterion, assumed that all peak voltages must be above 25 V. This model estimated that 38 percent of the peaks which would have been in the sample were less than 250 V and, therefore, were not observed. Figure 19 is a probability

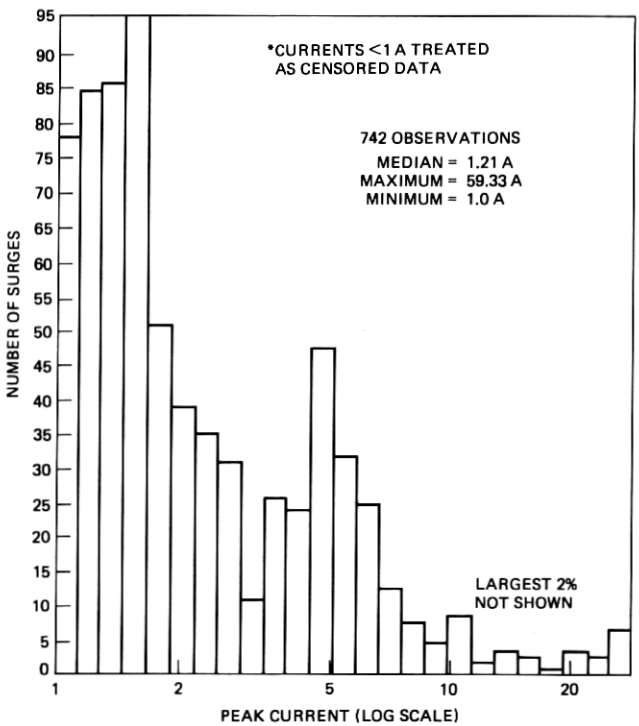

Fig. 20—Peak currents. Histogram of logs of peak current shown in units of amperes.

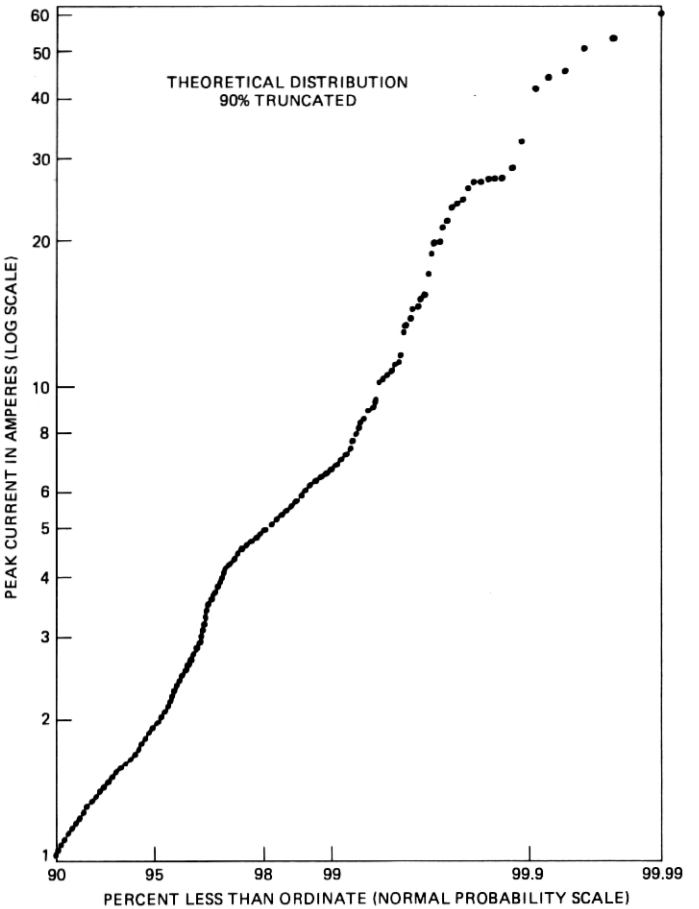

Fig. 21—Peak current assuming 90-percent truncation.

plot for the peak voltage data of this distribution. The total sample size, had all surges been measured, would have been 1983 (i.e., 1230 divided by [1-0.38]). This model would not be rejected by the K-S test at the 1 percent level, although it would be at the 5 percent level.

The parameters of the fitted theoretical distribution were $\mu = 5.57$ and $\sigma = 0.712$. (Units are in natural logarithms of [voltage -25].) The theoretical distribution in the original units of peak voltage would have a mean of 363 V, a median of 287, and a standard deviation of 274. The expected value of the smallest of 1983 observations is 50.2.

A.2 Peak current

Current waveforms were available for the 1230 surges on which voltage measurements were available. Peak current was defined for each of these as the absolute maximum current measured. A histogram

of logarithms of peak current is shown in Fig. 20. The scale is in logarithms of peak current because the original distribution was so skewed that little information could be obtained from plotting it. The largest 2 percent of the observations are not plotted. The maximum current recorded was 59.33 A. Forty percent of the surges fell into the "less than 1A" category and were used only to establish the median of 1.21 A.

All the distributions discussed in the previous section were also considered as models for the distribution of the 742 peak currents exceeding 1A. The best model was again a truncated lognormal distribution. A probability plot for observed peak current of the best-fitting lognormal distribution, one with 90 percent truncation, is shown in Fig. 21. Only a lower limit of 0 A was considered. This seemed reasonable because there were recorded observations nearly this small, although the reliability of such small observations was questionable. Although 90 percent of the observations are assumed to have been truncated in the best-fitting model, this percentage is not terribly unreasonable in view of the fact that 40 percent of the measured peaks were less than 1 A. In addition, it is not known how many surges not observed because their peak voltages were less than 250 V would have had peak currents less than 1 A. It should be noted that the 70- and 80-percent truncated distributions are also adequate models.

The best-fitting model had estimated parameters $\mu = -2.43$ and $\sigma = 1.89$. It would be accepted as an adequate fit at the 5 percent

Table I—Summary statistics for decay time constants and energy integrals

	Minimum	Maximum	Median	
Decay Time Constants				
$\frac{1}{v_p}\int \lvert v\rvert dt$	59.4	8543.5	436.0	μs
$\frac{1}{2v_p^2}\int v^2 dt$	28.1	13710.6	185.9	μs
$\frac{1}{i_p}\int \lvert i\rvert dt$	42.7	10312.4	694.2	μs
$\frac{1}{2i_p^2}\int i^2 dt$	18.2	19366.6	228.4	μs
Energy Integrals				
$\int \lvert v\rvert dt$	26908.	8924400.	181185.	volt-μs
$\int v^2 dt$	1060576.	7282113535.	16070750.	volt^2-μs
$\int \lvert i\rvert dt$	83.7	491798.	1618.	amp-μs
$\int i^2 dt$	23.0	25869386.	765.	amp^2-μs

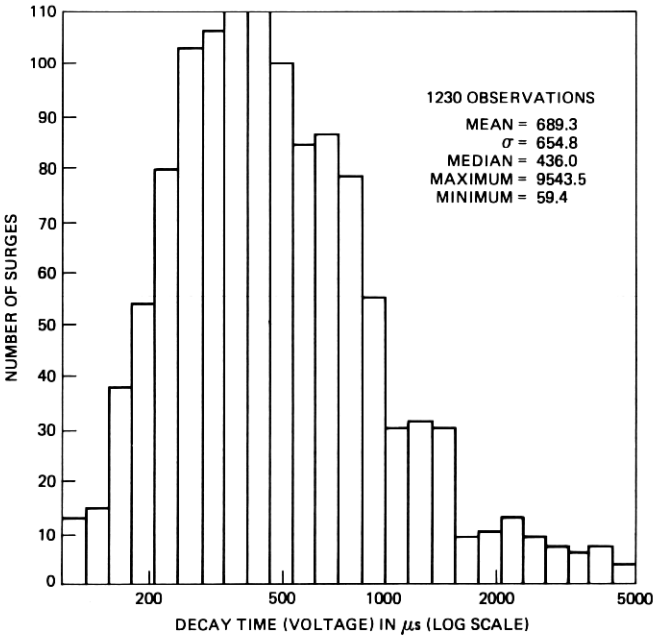

Fig. 22—Exponential equivalent decay time constant based on voltage magnitude. Histogram of logs of decay-time constant shown in units of microseconds.

significance level. The theoretical distribution in the original units of peak current would have a median peak current of 0.088 A, a mean of 0.52, and a standard deviation of 9.5 had all 7420 surges been observed.

A.3 Decay time and energy

The numerical integration necessary to compute equivalent decay time constants and related energy integrals from the waveforms involved summing trapezoidal areas between recorded data points. The integration was done from time $t = 0$ (which, in general, was the time at which the voltage exceeded the 250-volt trigger level*) to $t = 11.6$ ms. At 11.6 ms, the voltage or current was defined as 0, if the measurement had not previously reached a steady-state 0. (Non-zero values beyond the 11.6 ms point were generally measurement inaccuracies due to decreased resolution.)

Equivalent decay time constants were computed based on voltage (v), v^2, current (i), and i^2. (See formulas in Table I.) In addition, the value of each related energy integral was computed. The range of decay time constant based on voltage magnitude was from 60 to 8500

* In certain cases, the first oscilloscope data point occurred just prior to the time origin.

μs, and the median was 436.0 μs. Figures 22 and 23 are histograms of decay time constants for v and i, respectively. (Voltage is shown on a logarithmic scale.) Figures 9 and 10 in the text were plots of decay time constant based on v and v^2, respectively, versus a normal probability scale. A plot similar to Figs. 9 and 10 but for current (i) is in Fig. 24. The distributions of the four decay time variables were similar to each other, although those based on v^2 and i^2 had much longer tails than those based on v and i. Summary statistics for all decay time and energy distributions are shown in Table I.

Figure 25 is a graphical way of summarizing the decay time constant and energy data. Each box in the "box plot" (see Ref. 4) represents the distribution of one variable. The middle 50 percent of the data falls within the box. The horizontal lines represent the lower quartile, median, and upper quartile. "Whiskers" extend from the box to the minimum and maximum points. The decay time distributions appear surprisingly similar. The current distributions are more variable than the voltage distributions. This is perhaps accounted for by measurement discrepancies at the lower current levels. Also, the decay times

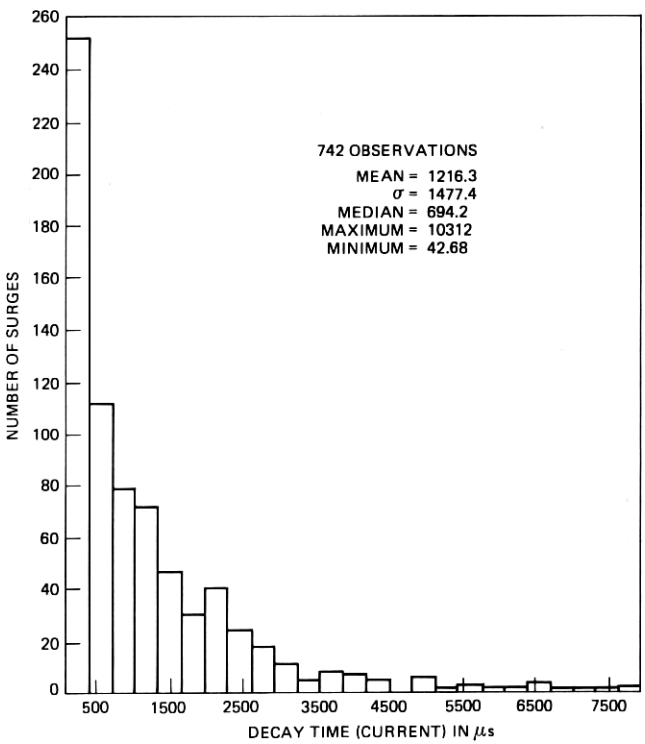

Fig. 23—Exponential equivalent decay-time constant based on current magnitude. Histogram of decay time constant shown in units of microseconds.

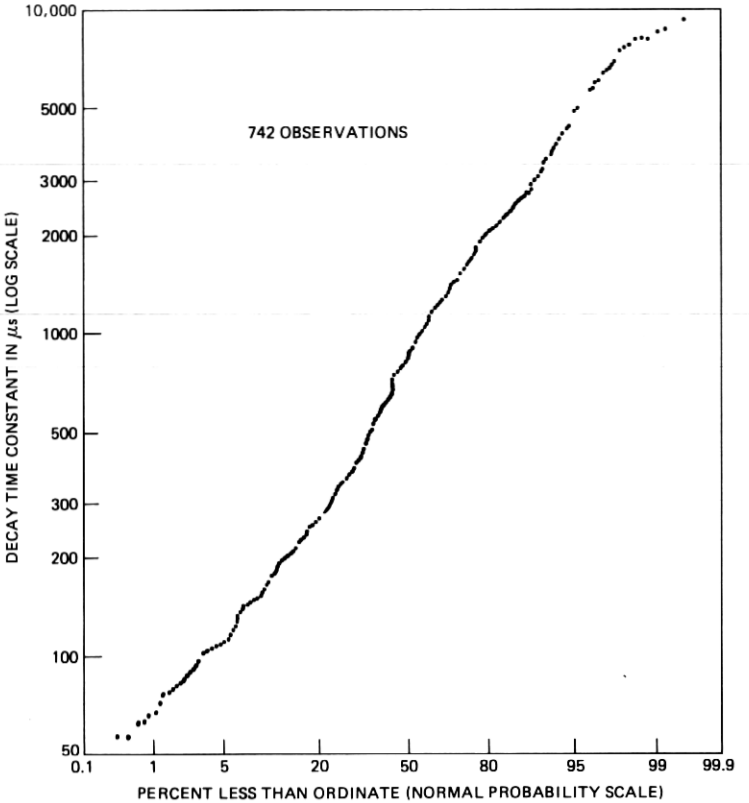

Fig. 24—Exponential equivalent decay-time constant based on current magnitude.

based on v^2 appear to be lower overall than those based on the other variables, and decay times for i are somewhat higher than for the others. The related energy integral distributions have different units (see Table I) and, therefore, appear quite different. The variability of all the distributions appears to be similar, however, on this logarithmic scale.

Since all the related energy integral distributions were similar to each other, an individual plot is included here for only one of these distributions. Figure 26 is a plot of the energy integral data for current (i) on a logarithmic scale versus a normal probability scale. Plots of the other energy integral distributions had shapes similar to Fig. 26, but, as noted previously, the scales are in different units.

Correlations were computed between decay time (based on voltage and voltage-squared) and peak voltage and between energy and peak voltage. This was likewise done for decay time and energy with peak current. Since decay time and/or energy is related to the stress imposed

on equipment, equipment ability to survive is frequently rated in terms of peak current or voltage and decay time constant. If large decay times occurred frequently in conjunction with high peaks, the effect of the combination would be worse for the equipment. All correlations computed were close to zero, except for those between energy (based on voltage and voltage-squared) and peak voltage. In both these cases, the correlation was slightly more than 0.4. One might expect that the equivalent decay times would *not* be correlated with peaks, because decay times are, in a sense, "standardized," since the area bounded by the waveform is divided by the peak value. (See formulas in Table I.)

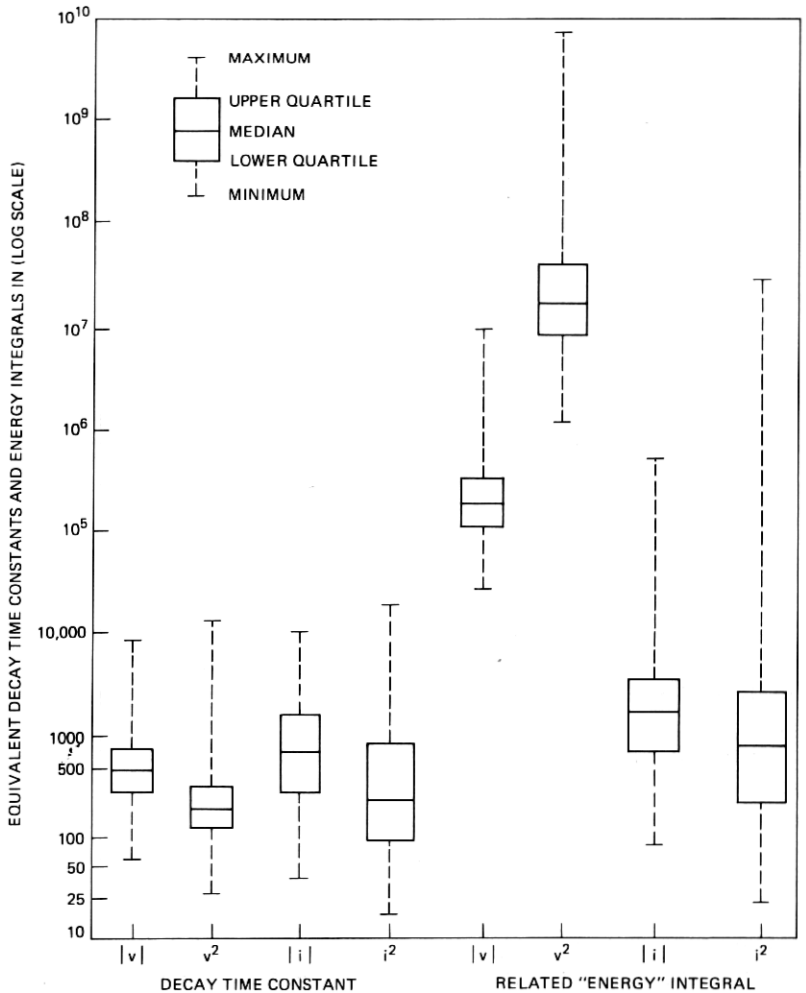

Fig. 25—"Box plot" representation of distributions of decay-time constants and energy integrals.

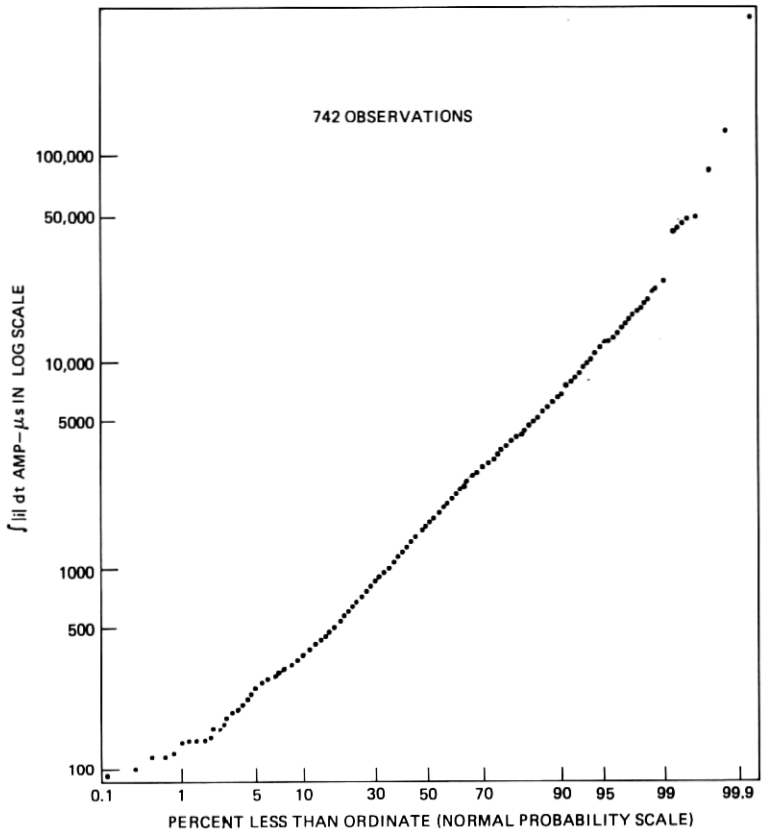

Fig. 26—Energy integral based on current magnitude.

The energy integrals are, however, equal to the decay time multiplied by the peak. Thus one would expect a correlation between energy and the corresponding peak. That this correlation is not found in the case of i or i^2 may be another indication of the imprecise nature of the current measurements. The correlation between peak voltages and the corresponding (v *and* v^2) energy integrals does, however, bear out this expectation.

REFERENCES

1. D. W. Bodle and P. A. Gresh, "Lightning Surges in Paired Telephone Cable Facilities," B.S.T.J., 40, No. 2 (March 1961), pp. 547–576.
2. E. Bennison, A. J. Ghazi, and P. Ferland, "Lightning Surges in Open Wire, Coaxial, and Paired Cables," International Conference on Communications, 1972.
3. M. A. Uman, *Lightning*, New York: McGraw-Hill, 1969.
4. J. W. Tukey, *Exploratory Data Analysis*, Reading, Mass.: Addison-Wesley, 1977.